INDOOR MODEL PROPELLER PERFORMANCE THEORY AND EVALUATION

Walter Lounsbery

INTRODUCTION

The results presented here are a small part of a project to achieve a working theoretical understanding of indoor model propellers, with an object of improved overall flight performance. Thus design is emphasized with high accuracy secondary. Three different design concepts are analyzed using this theory, the helical pitch, washed out blade tip, and cruise-optimized propeller types.

LIMITATIONS

As anyone involved in our hobby knows, there are limitations to any model. That statement is especially true to theoretical models or systems. In this paper, some limitations are:

1. Lack of hard data concerning the characteristics of indoor model airfoils.
2. Lack of compensation for tip "loss."
3. The assumption that pitching moment does not vary with thrust, which leads to the constant velocity theorem.

These limitations can be ignored only if we assume that airfoils of the type used on indoor models are insensitive to changes in Reynolds number (Ref. 4), and tip "loss" produces a very small error when the average blade loading is low (Ref. 5). The constant velocity theorem can be defended on the grounds that most indoor models are trimmed so that they fulfill the conditions of the theorem (one reason that they stall so easily on the power burst). Lastly, another source for inaccuracy is the set of airfoil characteristics used (Goettingen 417a, Ref. 3) which are only close to those used in indoor model props.

THEORY

The equations derived for these evaluations are different enough from the half-dozen or so sets of descriptions already out to warrant some explanation. Bascially, they are based on simple blade element theory using a different pitch definition. That is, pitch as used herein is **not** how far the prop will move forward in one revolution (or a single element) without slippage, but how far the prop actually moves forward. This formulation complicates the equation for blade angles, but simplifies the equations of thrust and torque. It follows that:

$$p=\frac{V}{RPS} \qquad \theta_k=\text{Arctan}\left(\frac{p}{2\pi r_k}\right)+\alpha_k$$

as shown in Appendix A, which also shows the vector components of lift and drag on this infinitesimal element of the blade. Utilizing the similar triangle of air velocities enables the equations for thrust and torque of the element to be written as:

$$dT=k\,C_D\,c\,(RPS)^2\left[\left(\frac{L}{D}\right)2\pi r-p\right]\cdot\sqrt{p^2+(2\pi r)^2}\,dr$$

$$dQ=k\,C_D\,c\,(RPS)^2\left[2\pi r+\left(\frac{L}{D}\right)p\right]r\cdot\sqrt{p^2+(2\pi r)^2}\,dr$$

The factor k is introduced to match the integrated torque equation to experimental value of torque required for cruise (eq. 7). It includes the density of air.

For most propellers solution of these equations must be carried out by numerical integration. In the one special case where chord is constant and the angle of attack is constant (as in the cruise-optimized prop during cruise) these equations can be evaluated with the techniques of calculus, giving these forms:

$$T=k\,b\,(RPS)^2\,C_D\,c\left[\frac{p}{2\pi}\left\{\frac{\left(\frac{L}{D}\right)(p^2+(2\pi r)^2)^{\frac{3}{2}}}{3p^3}-\frac{\pi r\sqrt{p^2+(2\pi r)^2}}{p^2}-\frac{1}{2}\ln\left(\frac{\sqrt{p^2+(2\pi r)^2}+2\pi r}{p}\right)\right\}\right]_{r_0}^{r_1}$$

$$Q=k\,b\,(RPS)^2\,C_D\,c\left[\left(\frac{p}{2\pi}\right)^2\cdot\left\{\frac{\pi r\left[(p^2+(2\pi r)^2)^{\frac{3}{2}}+\frac{3}{2}\sqrt{p^2+(2\pi r)^2}\right]}{2p^4}+\frac{\left(\frac{L}{D}\right)(p^2+(2\pi r)^2)^{\frac{3}{2}}}{3p^3}-\frac{1}{8}\ln\left(\frac{2\pi r+\sqrt{p^2+(2\pi r)^2}}{p}\right)\right\}\right]_{r_0}^{r_1}$$

which are less time consuming than numerical integration and much more accurate, usually.

In describing performance of propellers, an indispensible figure is efficiency, which is useful power out divided by power into a system. Here, considering only the blade itself, efficiency is

$$\frac{(dT)p}{\frac{(dQ)}{r}(2\pi r)}=\frac{\left[\left(\frac{L}{D}\right)2\pi r-p\right]p}{\left[2\pi r+\left(\frac{L}{D}\right)p\right]2\pi r}=\eta$$

This is a useful quantity, but if the propeller is viewed as a machine for changing torque into thrust, it will give no clue as to how effectively a prop is doing that job. Thus another quantity becomes necessary, the ratio of thrust to torque, which I shall call effectiveness (d). The more effective a propeller is, the smaller a motor is necessary.

Returning for the moment to the equation of thrust, it is a simple task to find the radius of zero thrust, or the minimum radius of useful blade area. Thrust is set to zero in equation 4 and the zero point is:

$$Z.P. = \frac{p}{(\frac{L}{D})2\pi}$$

Pitch is a very important variable in these equations. Anything that can be learned about how it varies in flight can simplify solutions quite a bit. Since pitch is related to the velocity of the model, one can approach it through the equations of flight to see how it behaves. These equations are derived in appendix B, and may be used to find percentage cruise thrust, lift, drag, or velocity in any phase of flight. This information is especially useful for flight profiling of indoor models, once the torque output of the motor is known and the thrust and torque equations of the prop are known.

The most significant result of these equations is that the velocity of a model is essentially constant. This has been referred to as the constant velocity theorem, which is applied to the thrust and torque equations to reduce the number of independent variables from two to one (RPS), and to simplify interpretation.

APPLICATION

Before applying this theory to the usual types of propellers, it is well to analyze the formulae themselves. It is evident that an indoor model spends much of its flight time in cruise or near-cruise (especially in low-ceiling flying), and further that the propeller design ought to be optimized for this condition. It can be seen from the formulae that the highest efficiency will be obtained when the airfoil is set to operate at its highest lift-to-drag ratio. It would also seem that the prop would be most effective when constructed in such a manner. For such a cruise-optimized prop, the equations for cruise simplify to:

$$d = \frac{\overline{[(\frac{L}{D})2\pi r - p]c}^{Av}}{\overline{[2\pi r + (\frac{L}{D})p]rc}^{Av}}, \quad \frac{L}{D} = \text{CONST.(MAX)}$$

$$\eta = \frac{\overline{[(\frac{L}{D})2\pi r - p]pc}^{Av}}{\overline{[2\pi r + (\frac{L}{D})p]2\pi rc}^{Av}}$$

$$\theta = \text{Arctan}(\frac{p}{2\pi r}) + \alpha, \quad \alpha = \text{CONST.}$$

For a typical airfoil alpha is usually around five to seven degrees for maximum L/D.

It is also well to use the theory to see what happens when some parameters are varied. This procedure is easy for the cruise-optimized propeller, and the graphs show the cruise characteristics of such props(figures 1 and 2). These trends apply to any type of prop, and show that there is a most effective and efficient blade area distribution, and that a higher pitch is more efficient while a lower pitch is more effective. In designing a propeller it will be noted that lower pitch results in higher rotational speed for a given thrust and velocity, and a lower torque input is required. The converse is true for higher pitches. Higher pitches require less blade area, also.

Using these equations for design takes a bit of trouble, but enables one to tailor the propeller to the model, instead of picking one which just **looks** like it will work. For most models one only needs to ballast the model and glide it to obtain the velocity, and then pick the desired cruise RPM. This determines the pitch, and reduces the design work to determining the area distribution for the desired thrust. The analysis becomes more complex if alpha is not constant. After a little experience, it is quite possible to determine the necessary cruise thrust from the glide test, since:

$$\frac{L}{D} = \cot\beta \quad ; \text{ glide test}$$

$$L = mg, \; D = \frac{D}{L}L \quad ; \text{cruise}$$

$$T = \frac{mg}{\cot\beta}$$

Once k is established, it will be simple to use this cruise thrust in the equations. My limited tests show k equal to 2.884×10^{-4} when cgs units are used.

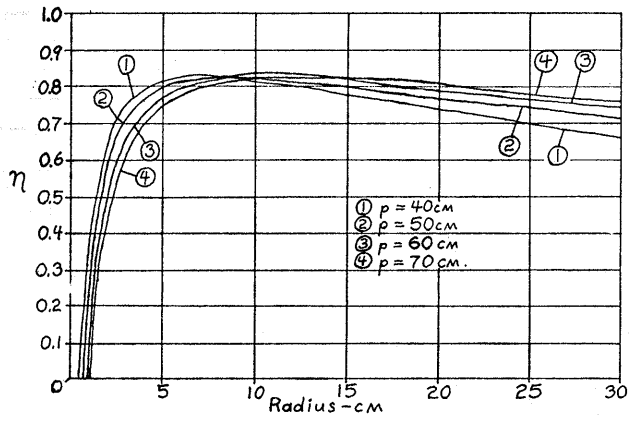

Figure 1. Efficiency, Radius, and Pitch

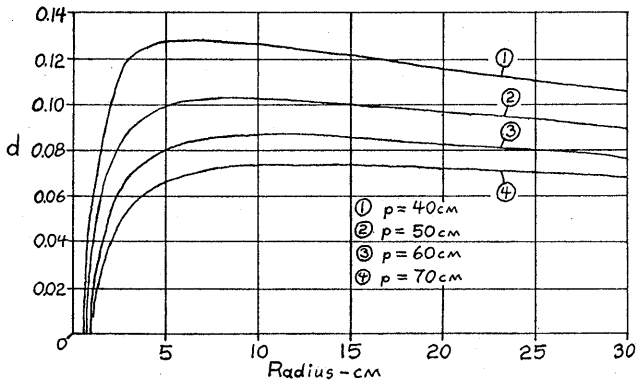

Figure 2. Effectiveness, Radius and Pitch

By the constant velocity theorem the only variable concerning the propeller in flight is rotational speed. For a picture of prop performance over the entire flight envelope, it is necessary to take many values of RPS to find the behavior of the propeller. This calculation is best done by computer, although, as it will be seen later, an easy approximation is obtainable. The results of the computation can show many important facts, as will be seen in the evaluations.

EVALUATION

One particularly successful and unusual propeller design was picked for the basis of these evaluations, the propeller used on Stan Chilton's G-3 paper stick model (Ref. 1). Unfortunately, as shown on the alpha distribution graph (Figure 4) of Chilton's prop, I underestimated Chilton's model. While the rotational speed in cruise is the figure published, it appears that the cruise velocity used (65 cm/sec), while typical of this class model, is not that of Chilton's model. Nevertheless, the comparisons will still be valid, and correction of the graphs needs only the substitution of the correct effective pitch for cruise, instead of the one indicated.

FIGURE 3

	G-3	Hel.	Optimized		
Rad.	Chord	Angle	Angle	Rad.	Chord	Angle
2.54	0	68.6	74.1	3.0	0	75.6
3.64	1.4	61.1	68.2	4.0	2.0	69.2
4.75	2.5	53.7	62.4	5.0	3.2	63.9
5.87	3.35	50.1	57.1	6.0	4.0	59.1
6.98	4.0	46.4	52.4	7.0	4.6	54.8
8.09	4.5	44.8	48.2	8.0	4.7	51.0
9.2	4.8	43.2	44.6	9.0	4.8	47.6
10.31	5.1	41.3	41.3	10.0	4.8	44.6
11.43	5.2	39.5	38.5	11.0	4.8	42.0
12.54	5.2	37.5	35.9	12.0	4.5	39.6
13.64	5.2	35.4	33.6	13.0	4.2	37.5
14.75	4.95	33.1	31.6	14.0	3.9	35.6
15.87	4.65	30.7	29.8	15.0	3.6	33.9
16.98	4.2	28.7	28.2	16.0	3.0	32.4
18.08	3.5	26.7	26.7	17.0	2.4	31.0
19.2	2.6	24.8	25.3	18.0	1.8	29.7
20.32	1.0	22.9	24.1	19.0	1.2	28.5

Two other propellers were designed for equivalent cruise thrust: a helical pitch propeller with the G-3 blade shape, and a cruise-optimized prop design. These props and the G-3 are described in figure 3. The performance evaluations were done on the University of Missouri's IBM 370-168 computer using the Goettingen 417a airfoil, which is close to indoor model airfoils.

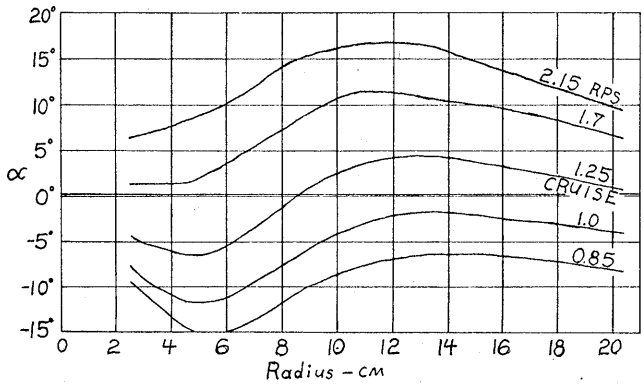

Figure 4. G-3 Angle of Attack

The physical and operational differences of these three propellers are shown very well in the alpha distribution graphs (figures 4, 5, and 6). It is somewhat surprising to note that on the helical and optimized props, there is a certain amount of relative washout at the blade tips as the props are driven at higher RPM than that for cruise. The outer tip of the helical version, indeed, does not vary more than a degree or two from the G-3, which would indicate that built-in washout is unnecessary. The G-3 also tends to "windmill" at the inside portion of the blade during descent.

The efficiency of the G-3 improves in climb, and drops off steeply in descent (figure 7). This characteristic is almost exactly copied by the equivalent helical-pitch propeller, which is actually more efficient by a small amount. The optimized prop shows even higher efficiency, and favors descent over climb (a good property considering the time spent in this phase of flight).

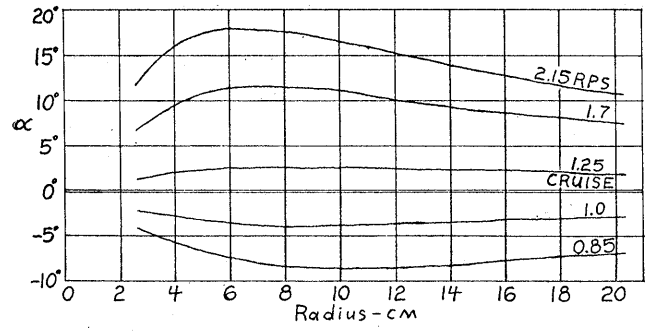

Figure 5. Hel. Prop Angle of Attack

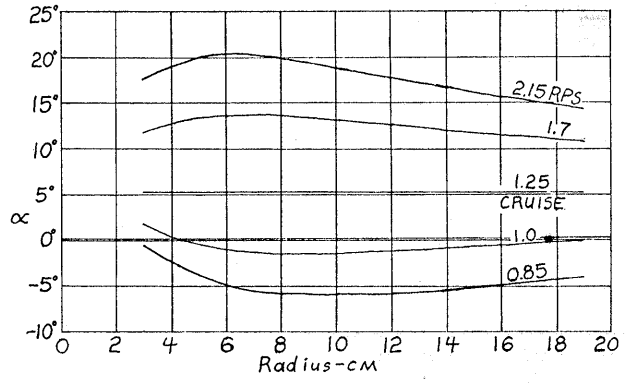

Figure 6. Opt. Prop Angle of Attack

It is interesting to see how the effectiveness of all three props increases with RPS (figure 8). The optimized prop, reasonably, ought not to follow this trend, having been optimized for cruise, but apparently the relative washout at the higher RPS increases the effectiveness to a certain extent. Again, the effectiveness of the G-3 and helical props drop sharply in descent, and the optimized prop favors descent.

The following graphs show just what has been hinted at until now; there are **simple** equations of thrust and torque (figures 9 and 10, and straight line equations at that. Although accuracy is not high, it is quite sufficient for comparisons to evaluate a design at 140% of cruise RPS and at 85% of cruise RPS, as well as at 100% done in the initial design work.

It can be seen that the helical pitch prop has the largest slope for its thrust and torque curves, followed by the G-3 and the optimized prop. This means that rotational speed of the helical prop is very "tight," varying little from cruise RPS. The G-3 has almost identical characteristics. The optimized prop is radically different, speeding up more in climb, and slowing down more in descent. This behavior might be considered good, considering that climb is short compared to cruise and descent, especially in ceilings under 50 feet. The efficiency during the cruise and descent must also be considered, however, as noted previously.

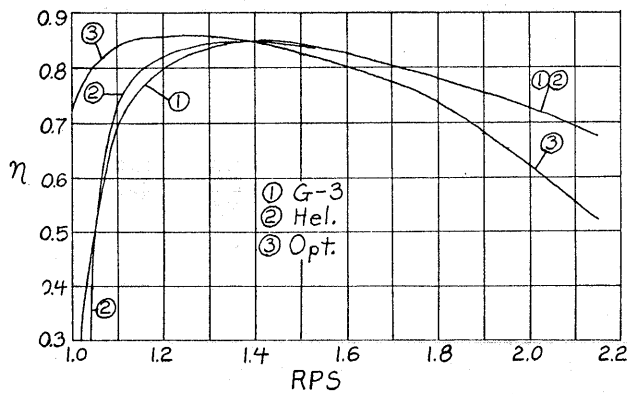

Figure 7. Efficiency

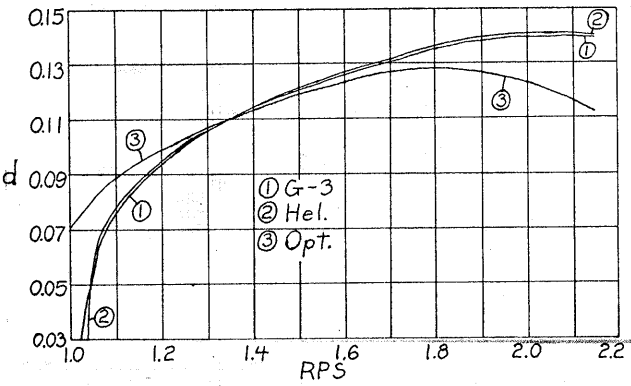

Figure 8. Effectiveness

The simple equations for percentage cruise thrust and torque are as follows:

G-3

RPS ≥ 1.25

$T\% = 360(RPS) - 450$

$Q\% = 240(RPS) - 200$

RPS ≤ 1.25

$T\% = 415(RPS) - 419$

$Q\% = 350(RPS) - 337.5$

Helical

RPS ≥ 1.25

$T\% = 364(RPS) - 355$

$Q\% = 240(RPS) - 200$

RPS ≤ 1.25

$T\% = 415(RPS) - 419$

$Q\% = 350(RPS) - 337.5$

Optimized

RPS ≥ 1.25

$T\% = 251(RPS) - 213$

$Q\% = 177(RPS) - 122$

RPS ≤ 1.25

$T\% = 325(RPS) - 306$

$Q\% = 280(RPS) - 250$

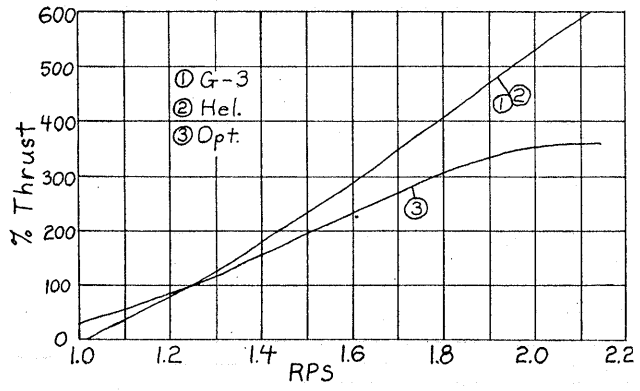

Figure 9. Percent Cruise Thrust

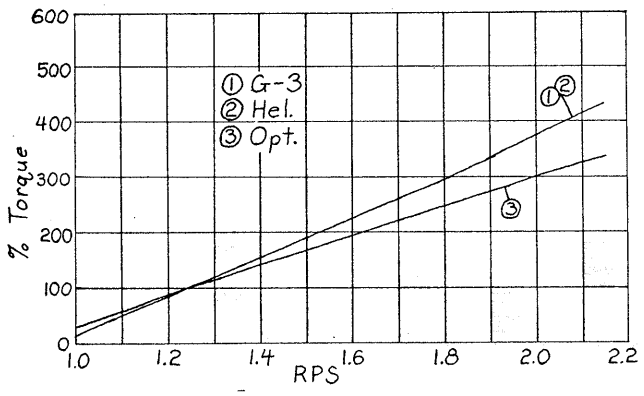

Figure 10. Percent Cruise Torque

These equations lead to approximations of the effectiveness, also. Unfortunately, there is no simple approximation for efficiency.

FURTHER WORK

Inasmuch as the theoretical side of indoor model propellers has been covered (excepting the limitations stated), the major work remaining is experimental. The propellers just may not behave as the theory developed here predicts. At any rate, a good value of k can only be obtained from experiments. One method to test props is to mount them on a device which will apply a variable, calibrated torque and measure the thrust output. This assembly can then be set on a horizontally rotating arm at a radius of two meters or so and set in motion to the desired airspeed.

Of course all this would only follow preliminary airfoil tests. Thus it is also necessary to construct a **sensitive** lift and drag balance, which could test wings while moving along a linear track. Additionally, such a device would offer great opportunity to develop good airfoils for indoor gliders and rubber models.

ACKNOWLDGEMENTS

I would like to thank the many people who have put up with this project, but most especially my parents, since it is **their** basement that is filled with models. In addition Roger Schroeder, Bill Langley, John Craig, Bud Tenney, and all the computer output handlers for their various criticisms and advice. This paper could be blamed on Dave Linstrum, also, for he suggested that it be submitted to the Symposium in the first place.

REFERENCES

1. STAN CHILTON-PLAN. P. 3, INDOOR NEWS AND VIEWS, MARCH-APRIL 1973.
2. WALTER S. DIEHL-ENGINEERING AERODYNAMICS, ROLAND PRESS CO., NEW YORK, 1928
3. NCAA ANNUAL REPORT NO. 286, P. 149, VOLUME 14, 1928.
4. TED OFF - "SOARING AND AERODYNAMICS," P. 23-25, 65, 66, MODEL BUILDER, FEBRUARY 1975.
5. GEORGE XENAKIS-"A COMPARISON OF "OPTIMUM" AND HELICAL-PITCH WAKEFIELD PROPELLERS," NFFS SYMPOSIUM REPORT, 1972.

SYMBOLS

b	number of blades
c	blade chord
C_D	airfoil coefficient of drag
d	effectiveness, T/Q
D	drag, dynes
g	980 cm/sec^2
k	unit constant
L	lift, dynes
m	mass, grams
n	efficiency, power out/power in
p	pitch, cm
Q	torque, dyne-cm
r	radius, cm
RPS	rotations per second
T	thrust, dynes
V	velocity of model, cm/sec
Z.P.	zero-point, cm
$\frac{L}{D}$	lift to drag ratio
α	blade angle of attack
β	angle of climb or descent
θ	blade angle to plane of rotation.

APPENDIX A

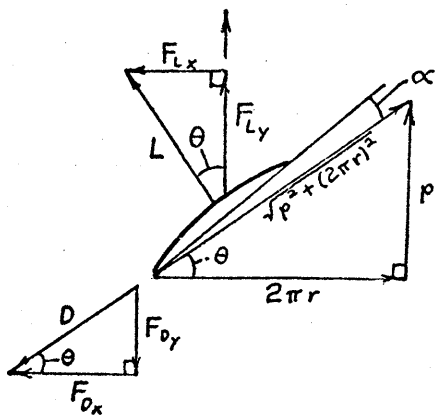

$$dD = C_D \rho c \left[p^2+(2\pi r)^2\right](RPS)^2 dr$$

$$dF_{Ly} = (dL)\cos\theta = (dL)\frac{2\pi r}{\sqrt{p^2+(2\pi r)^2}}$$
$$= \left[\left(\tfrac{1}{D}\right)2\pi r\right] C_D \rho c \sqrt{p^2+(2\pi r)^2}\,(RPS)^2 dr$$

$$dF_{Dx} = \left(\tfrac{D}{L}\right) dF_{Ly}$$

$$dF_{Lx} = (dL)\sin\theta = (dL)\frac{p}{\sqrt{p^2+(2\pi r)^2}}$$
$$= \left[\left(\tfrac{1}{D}\right)p\right] C_D \rho c \sqrt{p^2+(2\pi r)^2}\,(RPS)^2 dr$$

$$dF_{Dy} = \left(\tfrac{D}{L}\right) dF_{Lx}$$

$$dT = dF_{Ly} - dF_{Dy}$$
$$= \left[\left(\tfrac{1}{D}\right)2\pi r - p\right] C_D \rho c \sqrt{p^2+(2\pi r)^2}\,(RPS)^2 dr$$

$$dQ = (dF_{Lx} + dF_{Dx})r$$
$$= \left[2\pi r + \left(\tfrac{1}{D}\right)p\right] r\, C_D \rho c \sqrt{p^2+2\pi r)^2}\,(RPS)^2 dr$$

APPENDIX B

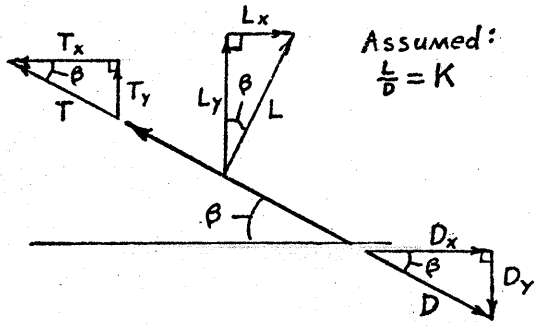

Assumed: $\frac{L}{D} = K$

$T_x = L_x + D_x \quad , T_y + L_y = D_y + mg$

$T\cos\beta = L\sin\beta + D\cos\beta$

$(T-D)\cos\beta = L\sin\beta$

$T\sin\beta + \left[\frac{(T-D)\cos\beta}{\sin\beta}\right]\cos\beta = D\sin\beta + mg$

$(T-D)\frac{1}{\sin\beta} = mg$

$T-D = mg\sin\beta$

$T = mg\sin\beta + D$

$T\cos\beta - D\cos\beta = L\sin\beta$

$mg\cos\beta = L$

$T = mg\sin\beta + D$

$T = mg(\sin\beta + \frac{D}{L}\cos\beta)$

Summary

$T = mg(\sin\beta + \frac{D}{L}\cos\beta)$

$D = \frac{D}{L}mg\cos\beta \quad , L = mg\cos\beta$

$T\% = \frac{L}{D}(\sin\beta + \frac{D}{L}\cos\beta)\cdot 100$

$D\% = L\% = \cos\beta \cdot 100$

$V\% = (\sqrt{\cos\beta})\cdot 100$